ELECTRO-PHOTO-INDUCED INTER-MINIBAND ABSORPTION STUDIES OF MULTI QUANTUM WELL SUPERLATTICES

J. OIKNINE-SCHLESINGER, M. GERLING, D. GERSHONI, E. EHRENFREUND, AND D. RITTER

Solid State Institute, Technion-Israel Institute of Technology, Haifa 32000, Israel.

We report the current induced intersubband absorption and the effect of external electric field on the mini-bands in the energy continuum of multi quantum well superlattices. We introduce a method by which, in n-i-n device, the steady state injected carrier density is directly measured, while applying bias voltage. We also show that already at relatively small electric fields, the continuum minibands merge into a single continuum band. This latter experimental observation is corroborated by 8 band $k \cdot p$ energy band calculations.

1 Introduction

In multi-quantum-well superlattices (MQWSL), states with energy considerably less than the barrier potential are degenerate and their wavefunctions are mostly confined within one period of the periodic structure. In contrast, states with energy greater than the barriers potential, form nondegenerate minibands of finite bandwidth, separated by forbidden minigaps in which the density of states strictly vanishes. In a previous work [1], we reported the observation of minibands within the energy continuum of such MQWSL. These minibands were spectroscopically observed by photoinduced intersubband absorption, in which the absorption due to optical transitions between the lowest photopopulated confined electron state to these minibands were measured.

Applying electric field, F, on MQWSL results in a relatively small blue shift of the transition between the confined states [2]. The effect on the continuum mini-bands (Cn) is more dramatic. Even at small F, the band bending causes a localization of the wavefunctions which results in merging of the Cn's to a single band. In this work we study electro-absorption (EA) and photoinduced absorption (PIA), at various F, of the transitions between two confined states (e1-e2) and between e1 and Cn, in an MQWSL structured n-i-n device. The e1-e2 EA yields a direct measure for the injection-current induced steady state population of e1. The e1-Cn PIA lines merge into the e1-e2 line with increasing F.

2 Experimental technique

The sample used is a n-i-n structure grown by metalorganic molecular beam epitaxy (MOMBE) [3] on a semi-insulating InP substrate, containing 25 periods of 60Å/300Å $In_{0.53}Ga_{0.47}As$ / InP undoped QW/barrier in its intrinsic region. The first

contact layer is a 3700Å n-doped InGaAs, followed by a 2000Å InP buffer layer. The second contact layer is a 900Å n-doped InGaAs, followed by a 800Å InP cap layer. The dimensions of the sample were determined by high resolution x-ray diffraction.

In order to apply electric field on the device, contacts were made to the doped regions using standard photolithographic techniques, resulting in one large mesa of $42mm^2$. The sample was fabricated as a multipass waveguide by polishing a 45^0 angle on both edges to allow for an IR electric field component along the growth direction. The PIA measurements were done utilizing the pump and probe technique [4], with an Ar^+ laser for the pump and a Nernst glower source for the probe. The sample was placed in a helium immersion cryostat with IR windows. All the measurements were done using a step-scan FTIR spectrometer where changes in the absorption due to induced electric field or photogenerated carriers were measured using standard lock-in technique.

3 Results and discussion

EA was measured at 6K, while applying a square voltage waveform on the device, at a frequency of 1.5kHz. The changes in the absorption due to F were measured for various positive and negative voltages (V). At each voltage, the carrier density was extracted from the e1-e2 EA by comparing it to the calculated absorption of the structure.

An Ohmic I-V characteristic is observed for this device, as shown in Fig. 1a. The current flowing through the device changes the population of the e1 level, giving rise to the e1-e2 "electro-absorption" observed in this device. The contribution of other electric field effects, in these low fields, is negligible. The integrated EA yields then the carrier density as explained above. The carrier density thus extracted is shown in Fig. 1a vs. V. We thus see that by measuring the e1-e2 EA, we determine the average well carrier density due to the injection current through the device. We believe it is the first direct method for measuring the current induced population in the well.

Furthermore, the ratio of the carrier density (as measured by EA) and the carrier flux (as extracted from I-V) is a measure for the average time a carrier spends in the well ("dwell time"). Fig. 1b shows the dwell time thus extracted as a function of V. As seen, the dwell time decreases mildly with increasing |V|. At 6K, the only effective carrier flow mechanism is by tunneling. Thus, as the electric field increases tunneling becomes easier, accounting qualitatively for the results. In order to account quantitatively for these results, we have calculated the width (Γ) of the resonant tunneling transmission probability through a barrier/well/barrier structure having the same dimensions as our device. Fig. 1b shows $\hbar/\Gamma$ thus calculated, as a solid line. As seen, except for very small positive V, the solid line

describes fairly well the data. We therefore conclude that by measuring I-V curves and EA in n-i-n (or similar) devices, we can obtain both the QW steady state population during current injection and the electronic dwell time in each well.

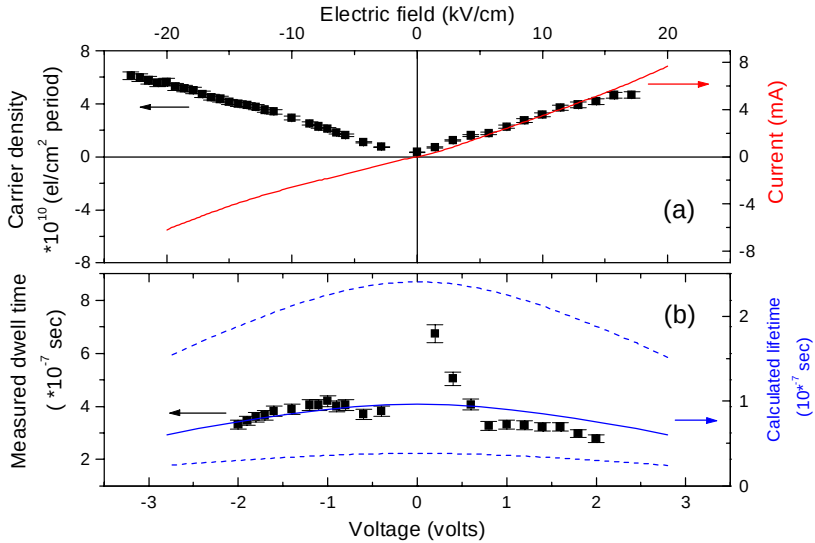

Figure 1. (a) Solid line: I-V curve of the device. Symbols: The measured carrier density vs. V. (b) Symbols: well dwell times for carriers vs. V. Solid line: The calculated $\hbar/\Gamma$ vs. V. Dashed lines: The uncertainty in the calculated lifetime due to 1 monolayer structural and 1% compositional uncertainty. The top scale gives the nominal electric field deduced from the applied voltage and the sample dimensions.

Fig. 2a shows the measured PIA spectra at various F. As can be seen the effect on the e1-Cn transitions is apparent even at very low fields. The tilted arrows show the evolution of three e1-Cn transitions, with F. All e1-Cn transitions are red shifted with F, merging eventually to a "single" relatively broad transition very close to the nearly unshifted e1-e2 transition. This behavior can readily be explained by calculating the device absorption spectra at different fields, as shown in Fig. 2b. For the calculations presented in Fig. 2b we have utilized 8 band $k \cdot p$ calculations under electric field [5]. Up to 10kV/cm, the blue shift of the e1-e2 transition is not noticeable. However, the transitions to the continuum are clearly affected, showing a red shift until merging with the e1-e2 transition. The inset shows the calculated bands for several electric fields. Already at 1 kV/cm, the induced band bending causes the formation of a Stark ladder and a noticeable localization of continuum electron wavefunctions. This localization reveals itself in the mixing of the second localized band e2 with the first mini-band in the

continuum, which results in the drastic change in the intersubband absorption spectrum.

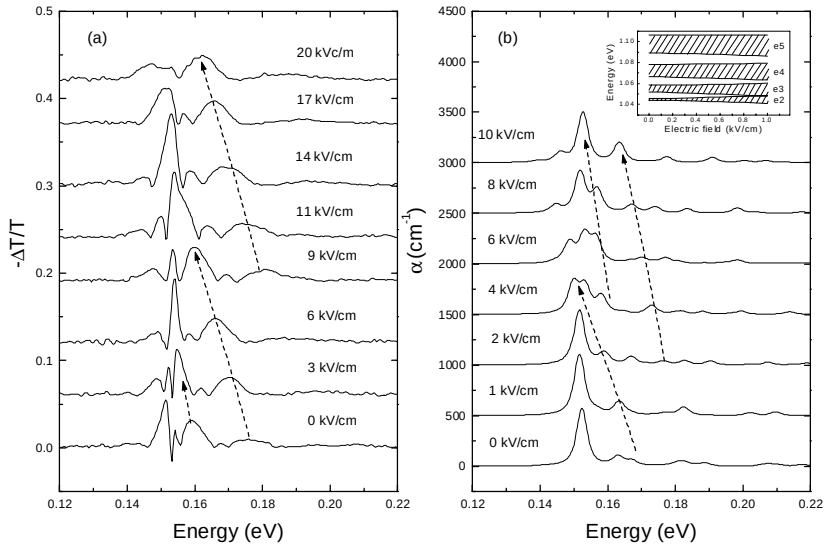

Figure 2.(a) The measured PIA for various applied fields. (b) The calculated e1-e2 and e1-Cn absorption spectra for various electric field strengths and for fixed carrier density of $4\times10^{10}/cm^2/period$. Inset: schematic view of the evolution of the minibands with applied electric field is shown in the inset. In both (a) and (b), the arrows indicate the red shifted e1-Cn transitions.

Acknowledgments: Work supported by the Israeli Science Foundation (184/97). The laboratories are under the auspices of the Center for Advanced Opto-Electronics in the Technion.

References

1. D. Gershoni, J Oiknine-Schlesinger, E. Ehrenfreund, D. Ritter, R.A. Hamm, M.B. Panish, *Phys. Rev. Lett.* **71** (1993) 2975.
2. A Harwit, J.S. Harris, *App. Phys. Lett.* **50** (1987) 685.
3. D. Ritter, R.A. Hamm, M.B. Panish, J.M. Vandenberg, D. Gershoni, S.D. Gunapala, B.F. Levine, *Appl. Phys. Lett.* **59** (1991) 552.
4. J. Oiknine-Schlesinger, E. Ehrenfreund, D. Gershoni, D. Ritter, M.B. Panish, R.A. Hamm, *Appl. Phys. Lett.* **62** (1991) 970.
5. M.E. Pistol, D. Gershoni, *Phys. Rev. B* **50** (1994) 738.